marine drugs

MDPI

Article

Butenolide Derivatives with α-Glucosidase Inhibitions from the Deep-Sea-Derived Fungus *Aspergillus terreus* YPGA10

Zhongbin Cheng [1,†], Yuanli Li [1,†], Wan Liu [1], Lijun Liu [1], Jie Liu [1], Wangjun Yuan [1,*], Zhuhua Luo [2], Wei Xu [2,*] and Qin Li [1,3,*]

1 Pharmaceutical College, Henan University, Kaifeng 475004, China; czb360@126.com (Z.C.); lyl328743993@163.com (Y.L.); 18737806806@163.com (W.L.); 15736871748@163.com (L.L.); ll18737801136@163.com (J.L.)
2 Key Laboratory of Marine Biogenetic Resources, Third Institute of Oceanography, Ministry of Natural Resources, Xiamen 361005, China; luozhuh@tio.org.cn
3 Eucommia Ulmoides Cultivation and Utilization of Henan Engineering Laboratory, Kaifeng 475004, China
* Correspondence: yuanwangjun@henu.edu.cn (W.Y.); xuwei@tio.org.cn (W.X.); liqin6006@163.com (Q.L.); Tel.: +86-371-2388-3849 (Q.L.)
† These authors contributed equally to this work.

Received: 15 May 2019; Accepted: 31 May 2019; Published: 3 June 2019

Abstract: Three new butenolide derivatives, namely aspernolides N–P (**1**–**3**), together with six known analogues (**4**–**9**), were isolated from the ethyl acetate (EtOAc) extract of the deep sea-derived fungus *Aspergillus terreus* YPGA10. The structures of compounds **1**–**3** were determined on the basis of comprehensive analyses of the nuclear magnetic resonance (NMR) and mass spectroscopy (MS) data, and the absolute configurations of **1** and **2** were determined by comparisons of experimental electronic circular dichroism (ECD) with calculated ECD spectra. Compound **1** represents the rare example of *Aspergillus*-derived butenolide derivatives featured by a monosubstituted benzene ring. Compounds **6**–**9** exhibited remarkable inhibitory effects against α-glucosidase with IC_{50} values of 3.87, 1.37, 6.98, and 8.06 μM, respectively, being much more active than the positive control acarbose (190.2 μM).

Keywords: *Aspergillus terreus* YPGA10; deep-sea-derived fungus; butenolide derivatives; α-glucosidase

1. Introduction

Butyrolactone derivatives from the fungal genera *Aspergillus* are a group of natural products usually consisting of three moieties: An α,β-unsaturated-γ-lactone moiety and two phenyl moieties. These are mainly produced by the species *Aspergillus terreus*. Since butyrolactone I was first reported in 1907, dozens of analogues have been isolated and characterized from the fungal genera *Aspergillus* [1–11]. Some members exhibited significant bioactivity, such as anti-neuroinflammatory activity [5,8], α-glucosidase inhibitory activity [9,10], antiplasmodial activity [7], and antibacterial activity [7]. In recent years, deep-sea fungi have been well recognized as a rich source of secondary metabolites endowed with unusual structures and significant bioactivities [12]. As part of our ongoing efforts to discover bioactive molecules from deep-sea derived fungi [13–17], an EtOAc extract of a fungal strain *Aspergillus terreus* YPGA10 displayed the ^{1}H NMR resonances similar to those of butyrolactone I. A bioassay revealed that the EtOAc extract possessed an inhibition rate of 67% at a single dose (100 μg/mL) against α-glucosidase. Subsequent chromatography of the EtOAc fraction yielded three new butenolide derivatives, namely aspernolides N–P (**1**–**3**), along with six known analogues (**4**–**9**) (Figure 1). All compounds were tested for their inhibitory activities against α-glucosidase. Herein,

the details of the isolation, structural elucidation, and the α-glucosidase inhibitory activities of **1**–**9** are described.

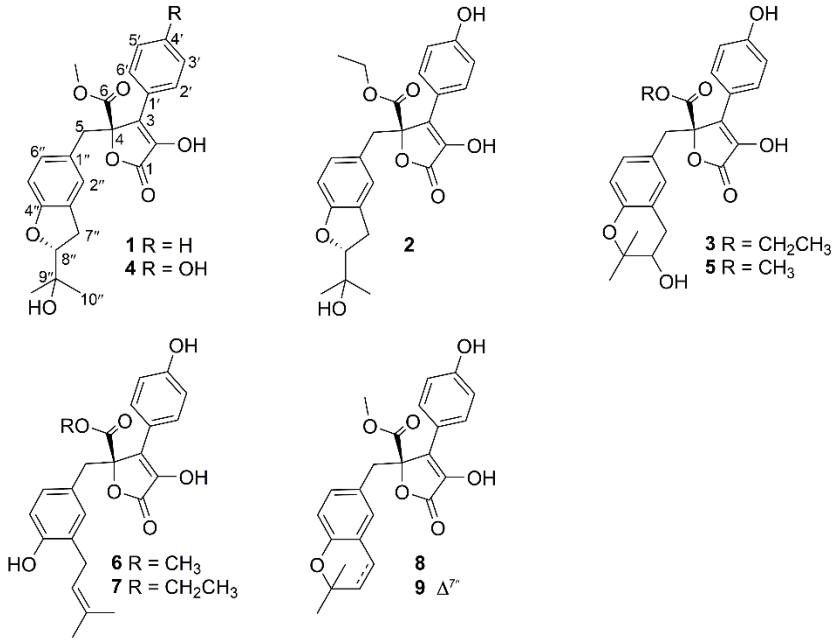

Figure 1. Structures of compounds **1**–**9** from *Aspergillus terreus* YPGA10.

2. Results

Compound **1** had a molecular formula of $C_{24}H_{24}O_7$, as established by the high-resolution electrospray ionization mass spectroscopy (HRESIMS) and nuclear magnetic resonance (NMR) data (Table 1), requiring thirteen degrees of unsaturation. The ^{1}H NMR spectrum (Figure S1) provided signals for two methyls (δ_H 1.19, s; 1.16, s), a methoxyl (δ_H 3.79, s), an oxygenated methine [δ_H 4.50 (dd, J = 9.3, 8.6 Hz, 1H)], a 1,3,4-trisubstituted benzene ring [δ_H 6.59 (d, J = 1.6 Hz, 1H); 6.45 (d, J = 8.2 Hz, 1H); 6.52 (dd, J = 8.2, 1.6 Hz, 1H)], a monosubstituted benzene ring [δ_H 7.70 (dd, J = 8.4, 1.2 Hz, 2H); 7.46 (dd, J = 8.4, 7.4 Hz, 2H); 7.37 (dd, J = 7.4, 1.2 Hz, 1H)], and two methylenes (δ_H 2.99, m; 3.49, s). While the ^{13}C NMR and the heteronuclear single quantum coherence (HSQC) spectra (Figures S2 and S3) exhibited 24 carbon resonances attributable to two benzene rings (δ_C 132.1, 128.5, 128.5, 129.8, 129.8, 129.6, 126.2, 127.9, 128.1, 160.5, 109.1, 131.0), a double bond [δ_C 128.1, C-2 (not detected)], two carbonyls (δ_C 170.3, 171.5), two methylenes (δ_C 39.6, 31.3), a methoxy group (δ_C 53.9), an oxygenated methine (δ_C 90.4), and a oxygenated tertiary carbon (δ_C 72.5). The ^{1}H and ^{13}C NMR data in association with the heteronuclear multiple bond correlation (HMBC) correlations established a butenolide derivative, structurally related to a co-isolated known compound butyrolactone IV (**4**) [6]. The only difference was owing to the presence of a monosubstituted benzene ring in **1** instead of the 1,4-disubstituted benzene ring in **4**. The structure of **1** was further secured by detailed analyses of the 2D NMR data (Figure 2). In order to assign the absolute configuration, the ECD calculation was performed at the b3lyp/6-31+g(d,p) level in methanol using the b3lyp/6-31+g(d,p)-optimized geometries for the four possible model molecules. The theoretical ECD spectra for (4*R*, 8″*R*)-**1**, (4*R*, 8″*S*)-**1**, and their enantiomers were calculated by the time-dependent density functional theory (TDDFT) method. Comparison of the experimental CD curve of **1** with the computed ECD curves (Figure 3) indicated the absolute configurations of **1** to be 4*R* and 8″*R*. The absolute configuration of **1** was supported by possessing similar specific rotation and CD spectrum to those of **4**, whose structure was established by X-ray single-crystal diffraction experiment [6]. Compound **1**, featured by a monosubstituted benzene ring, was rarely found in this class of butenolide derivatives and was named aspernolide N.

Table 1. ^{1}H and ^{13}C NMR Data of **1**–**3** in Methanol-d_4 [a].

No.	1		2		3	
	δ_H	δ_C	δ_H	δ_C	δ_H	δ_C
1		170.3		170.5		170.7
2		not detected		140.0		140.2
3		128.1		129.1		129.0
4		86.9		86.9		86.9
5	3.49, s	39.6	3.46, s	39.7	3.44, s	39.5
6		171.5		171.0		171.0
1′		132.1		123.2		123.3
2′, 6′	7.70, dd (8.4, 1.2)	128.5	7.60, d (8.9)	130.4	7.59, d (8.7)	130.3
3′, 5′	7.46, dd (8.4, 7.4)	129.8	6.87, d (8.9)	116.6	6.87, d (8.7)	116.5
4′	7.37, dd (7.4, 1.2)	129.6		159.3		159.2
1″		126.2		126.3		126.2
2″	6.59, d (1.6)	127.9	6.61, d (1.5)	127.9	6.48, d (1.8)	132.9
3″		128.1		128.0		120.5
4″		160.5		160.4		153.4
5″	6.45, d (8.2)	109.1	6.46, d (8.2)	109.1	6.48, d (8.2)	117.2
6″	6.52, dd (8.2, 1.6)	131.0	6.54, dd (8.2, 1.5)	131.0	6.56, dd (8.5, 1.8)	130.4
7″	2.99, m	31.3	2.99, m	31.3	2.77, dd (16.6, 5.4); 2.53, dd (16.6, 7.5)	32.0
8″	4.50, dd (9.3, 8.6)	90.4	4.49, dd (9.3, 8.6)	90.4	3.67, dd (7.5, 5.4)	70.4
9″		72.5		72.5		77.9
10″	1.19, s	25.2	1.19, s	25.2	1.27, s	25.8
11″	1.16, s	25.3	1.16, s	25.3	1.17, s	20.9
$OCH_{2/3}$	3.79, s	53.9	4.25, q (7.1)	63.7	4.25, q (7.0)	63.7
CH_3			1.21, t (7.1)	14.2	1.21, t (7.0)	14.2

[a] ^{1}H NMR recorded at 400 MHz, ^{13}C NMR recorded at 100 MHz.

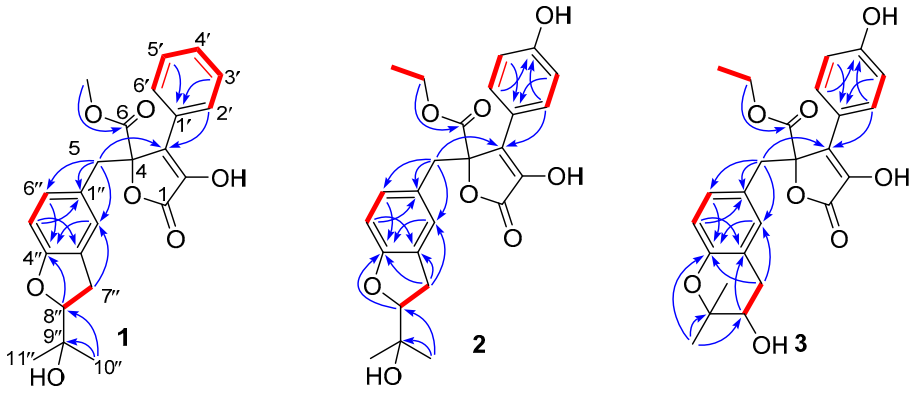

Figure 2. Key correlation spectroscopy (COSY) and heteronuclear multiple bond correlation (HMBC) of **1**–**3**.

Compound **2** had a molecular formula of $C_{25}H_{26}O_8$, as established by the HRESIMS data (Figure S28), requiring 13 degrees of unsaturation. The ^{1}H NMR and ^{13}C NMR data (Table 1) were almost identical with those of **4**, with the only distinction attributable to the presence of an ethoxy group [δ_H 4.25 (2H, q, J = 7.1 Hz), 1.21 (3H, t, J = 7.1 Hz); δ_C 63.7] in **2** instead of the methoxy group [δ_H 3.76 (3H, s); δ_C 53.9] in **4**. The linkage of the ethoxy group to C-6 was deduced by the COSY relationship between the methyl protons (δ_H 1.21) and the oxygenated methyene protons (δ_H 4.25) in combination with the HMBC correlations from the methyene protons (δ_H 4.25) to the carbonyl carbon C-6 (δ_C 171.0) (Figure 2). Comparison of the experimental ECD spectra with the calculated ECD data for the model molecules (4*R*,8″*R*; 4*S*,8″*S*; 4*R*, 8″*S*; 4*S*, 8″*R*) allowed the assignment of the 4*R* and 8″*R* configurations for **2** (Figure 4).

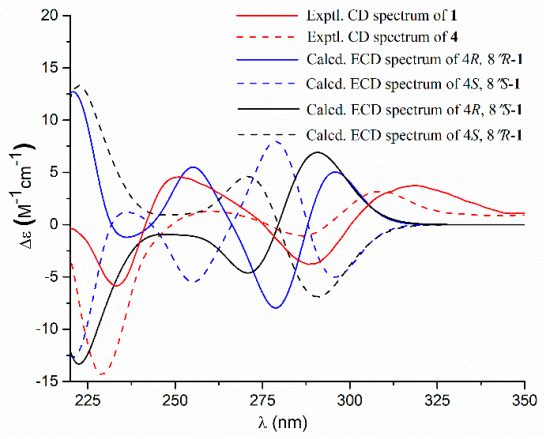

Figure 3. Experimental and calculated electronic circular dichroism (ECD) spectra of **1** and experimental ECD spectrum of **4** in methanol.

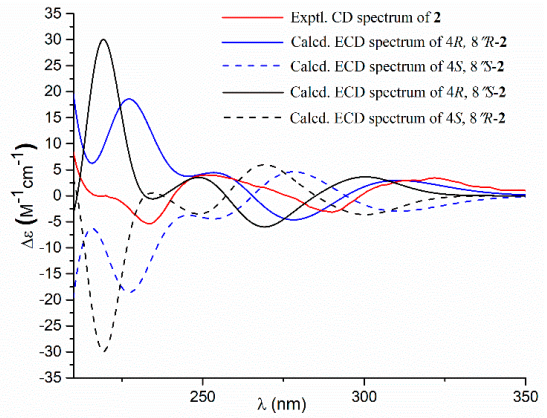

Figure 4. Experimental and calculated electronic circular dichroism (ECD) spectra of **2** in methanol.

Compound **3** had a molecular formula of $C_{25}H_{26}O_8$, as established by the HRESIMS data (Figure S29), requiring 13 degrees of unsaturation. The ^{1}H NMR and ^{13}C NMR data (Table 1) provided the characteristic resonances for a 1,3,4-trisubstituted benzene ring, a 1,4-disubstituted benzene ring, and an α,β-unsaturated-γ-lactone group. Analyses of the 2D NMR spectra conducted **3** to be an analogue of a co-isolated known compound butyrolactone V (**5**) [18]. The difference was found by the presence of an ethoxy group [δ_H 4.25 (2H, q, J = 7.0 Hz), 1.21 (3H, t, J = 7.0 Hz); δ_C 63.7] in **3** instead of the methoxy group [δ_H 3.78 (3H, s); δ_C 53.9] in **5**. The ethoxy group was located at C-6 by the HMBC correlations from the oxygenated methyene protons (δ_H 4.25) to the carbonyl carbon C-6 (δ_C 171.0). The structure of **3** was further secured by detailed analyses of 2D NMR data (Figure 2). The abosulte configuration of C-4 was proposed to be *R*, the same as that of **5,** based on their almost identical CD spectra (Figure 5). Compound **3** was given the trivial name aspernolide P.

In addition, six additional known compounds were identical to butyrolactone IV (**4**) [6], butyrolactone V (**5**) [18], butyrolactone I (**6**) [3], butyrolactone VII (**7**) [7], aspernolide A (**8**) [1], and aspernolide E (**9**) [2] based on comparisons of their NMR data (Figures S16–S26) and specific rotations with those reported in the literature.

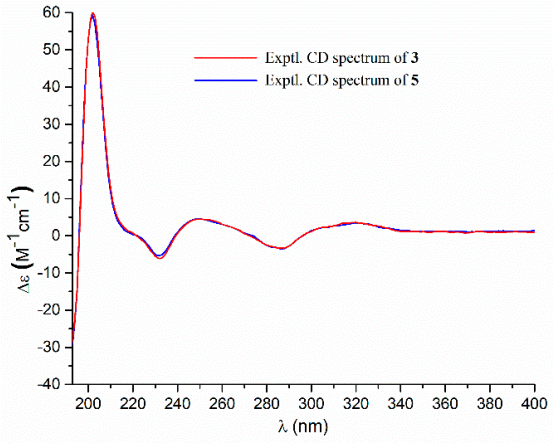

Figure 5. Experiment ECD spectra of **3** and **5** in methanol.

As the extract exhibited strong inhibitions against α-glucosidase, and the literature suggested that some members of this class of butyrolactone derivatives possessed significant inhibitions against α-glucosidase [9,10]. Thus, all compounds were screened for their inhibitory activities against α-glucosidase (Table 2) at the initial concentration of 100 μM. Compounds **6**–**9** with inhibitions more than 50% were further evaluated to calculate the IC_{50} values (Table 2). The results showed that compounds **6**–**9** were strong inhibitors with IC_{50} values ranging from 1.37 to 8.06 μM, being more active than the positive control acarbose (190.2 μM). The structural variability of this series of butyrolactone derivatives and their inhibitory activity toward α-glucosidase in our study may define some structure-activity relationship: (a) The ethoxyl group at C-6 may lead to a small increase of the activity than methoxyl group, as compound **7** was 2-fold more active than compound **6**. (b) The $\Delta^{7''}$ of the pyran ring may have negligible effects on the activity, as compound **9** possessed similar activity to its hydrogenated derivative **8**. (c) The introduction of a hydroxy group at C-8″ of the pyran ring may lead a sharp decrease in activity, as compound **8** exhibited significant inhibition at 100 μM, while its 8″-hydroxylated derivative **5** showed negligible inhibitory activity at the same concentration.

Table 2. Inhibitory Effects of the Compounds on α-Glucosidase.

No.	%Inhibition (100 μM)	IC_{50} (μM)
1	18.62	- [c]
2	23.18	- [c]
3	26.43	- [c]
4	37.29	- [c]
5	21.57	- [c]
6	100/89.41 [b]	3.87 ± 0.33
7	100/98.69 [b]	1.37 ± 0.05
8	89.17	6.98 ± 0.22
9	90.43	8.06 ± 0.21
Acarbose [a]		190.2 ± 2.4

[a] Positive control. [b] 50 μM. [c] Not tested.

The α-glucosidase inhibitory activities of **1**–**3**, **7**, and **9** were evaluated for the first time, and the preliminary structure−activity relationship may provide information for further structural optimization of these α-glucosidase inhibitors.

3. Experimental Section

3.1. General Experimental Procedure

Specific rotations were measured by an SGW®-1 automatic polarimeter (Shanghai Jing Ke Industrial Co., Ltd., Shanghai, China). Ultraviolet (UV) spectra were measured on a UV-2600 spectrometer. ECD spectra were measured on an Aviv Model 420SF spectropolarimeter (Aviv Biomedical Inc., Lakewood, CA, USA). The NMR spectra were recorded on a Bruker Avance III HD-400 spectrometer (Bruker, Fällanden, Switzerland). HRESIMS spectra were obtained on a Waters Xevo G2 Q-TOF spectrometer (Waters Corporation, Milford, MA, USA). Semi-preparative high-performance liquid chromatography (HPLC) was undertaken on a Shimadzu LC-6AD pump (Shimadzu Co., Kyoto, Japan) using a UV detector, and a YMC-Pack ODS-A HPLC column (semipreparative, 250 × 10 mm, S-5 μM, 12 nm, YMC Co., Ltd., Kyoto, Japan) was used for separation.

3.2. Fungal Strain and Identification

Fungus *Aspergillus terreus* YPGA10 was isolated from the deep-sea water at a depth of 4159 m in the Yap Trench (West Pacific Ocean). The strain was identified as *Aspergillus terreus* based on microscopic examination and by internal transcribed spacer (ITS) sequencing. The ITS sequence has been deposited in GenBank (http://www.ncbi.nlm.nih.gov) with accession number MG835907. The strain YPGA10 (MCCC3A01013) was deposited at the Marine Culture Collection of China.

3.3. Fermentation

The fermentation was carried out in 40 Fernbach flasks (500 mL), each containing 80 g of rice. Distilled water (90 mL) was added to each flask, and the contents were soaked for 3 h before autoclaving at 15 psi for 30 min. After cooling to room temperature, each flask was inoculated with 3.0 mL of the spore inoculum and incubated at room temperature for 30 days.

3.4. Extraction and Isolation

The fermented materials were extracted with EtOAc (3 × 2000 mL) in an ultrasonic bath at 25 °C for 30 min. After evaporation under vacuum, the EtOAc extract (12.0 g) was subjected to ODS silica gel column chromatography (CC) eluting with MeOH/H_2O (20:80→100:0) to afford 10 fractions (F1–F10). F7 was further chromatographed over C-18 silica gel CC eluted with MeOH/H_2O (65:35) to afford 7 subfractions (F7a–F7g). F7d was further purified by HPLC on a semi-preparative YMC-pack ODS-A column using MeOH/H_2O (65:35, 2 mL/min) to afford **7** (71 mg, t_R 45 min). F7e was separated by HPLC using MeOH/H_2O (67:33, 2 mL/min) to give **1** (1.4 mg, t_R 44 min). F7f was separated by HPLC using ACN/H_2O (57:43, 2 mL/min) to obtain **8** (31 mg, t_R 65 min) and **9** (1.4 mg, t_R 57 min). F6 was subjected to sephadex LH-20 (MeOH) to obtain F6a–F6e and **6** (1.8 g). F6b was further chromatographed over C-18 silica gel CC eluted with MeOH/H_2O (40%, 50%, 60%, 70%, 80%, 90%, 100%) to give F6b1–F6b5. F6b1 was separated by HPLC eluted with ACN/H_2O (50:50, 2 mL/min) to afford **4** (101 mg, t_R 43 min). F6b2 was chromatographed by HPLC using ACN/H_2O (51:49, 2 mL/min) as eluent to obtain **3** (7 mg, t_R 44 min) and **2** (10 mg, t_R 46 min). F6b3 was purified by HPLC eluted with ACN/H_2O (47:53, 2 mL/min) to afford **5** (23 mg, t_R 38 min).

Aspernolide N (**1**): Colorless oil; $[\alpha]_D^{25}$ +59 (*c* 0.03, MeOH); UV (MeOH) λ_{max} (log ε) 201 (4.39), 287 (3.73) nm; ECD (*c* 2.8 × 10^{-4} M, MeOH) λ_{max} ($\Delta\varepsilon$) 286 (−1.09), 229 (−14.39), 202 (+43.55); ^{1}H and ^{13}C NMR data, see Table 1; HRESIMS *m*/*z* 447.1403 $[M + Na]^+$ (calcd. for $C_{24}H_{24}O_7Na^+$, 447.1414).

Aspernolide O (**2**): Colorless oil; $[\alpha]_D^{25}$ +63 (*c* 0.16, MeOH); UV (MeOH) λ_{max} (log ε) 226 (4.15), 306 (4.33) nm; ECD (*c* 2.2 × 10^{-4} M, MeOH) λ_{max} ($\Delta\varepsilon$) 290 (−3.16), 251 (+3.99), 235 (−5.35), 202 (+47.49); ^{1}H and ^{13}C NMR data, see Table 1; HRESIMS *m*/*z* 477.1525 $[M + Na]^+$ (calcd. for $C_{25}H_{26}O_8Na^+$, 477.1520).

Aspernolide P (**3**): Colorless oil; $[\alpha]_D^{25}$ +73 (*c* 0.14, MeOH); UV (MeOH) λ_{max} (log ε) 226 (4.33), 306 (4.43) nm; ECD (*c* 2.1 × 10^{-4} M, MeOH) λ_{max} ($\Delta\varepsilon$) 286 (−3.32), 249 (+4.45), 232 (−6.16), 202 (+60.34); ^{1}H and ^{13}C NMR data, see Table 1; HRESIMS *m*/*z* 477.1518 $[M + Na]^+$ (calcd. for $C_{25}H_{26}O_8Na^+$, 477.1520).

Butyrolactone IV (**4**): ECD (*c* 2.2 × 10^{-4} M, MeOH) λ_{max} ($\Delta\varepsilon$) 288 (−3.78), 233 (−5.86), 203 (+48.20).

Butyrolactone V (**5**): ECD (*c* 2.8 × 10^{-4} M, MeOH) λ_{max} ($\Delta\varepsilon$) 286 (−3.50), 249 (+4.61), 232 (−5.31), 202 (+59.41).

3.5. Computation Section

In general, conformational analyses were carried out via random searching in the Sybyl-X 2.0 [19] using the MMFF94S force field with an energy cutoff of 2.5 kcal/mol. Subsequently, the conformers were re-optimized using density functional theory (DFT) at the b3lyp/6-31+g(d,p) level in MeOH using the polarizable conductor calculation model by the GAUSSIAN 09 program [20]. The energies, oscillator strengths, and rotational strengths (velocity) of the first 30 electronic excitations were calculated using the TDDFT methodology at the rcam-b3lyp/6-31+g(d,p) level in MeOH. The ECD spectra were simulated by the overlapping Gaussian function (half the bandwidth at 1/e peak height, σ = 0.16 for (4*R*, 8′′*R*) and (4*R*, 8′′*S*)-**1**, 0.30 for (4*R*, 8′′*R*)-**2**, and 0.2 for (4*R*, 8′′*S*)-**2**). By comparing the experiment spectra with the calculated ECD spectra, the absolute configurations of **1** and **2** were resolved.

3.6. α-Glucosidase Assay

The *α*-glucosidase inhibitory effect was assessed using a previously described method with slight modification [21,22]. 0.2 U of *α*-glucosidase from *Saccharomyes cerevisiae* purchased from Sigma-Aldrich (St. Louis, MO, USA) was diluted to 0.1 M phosphate buffer consisting of Na_2HPO_4 and NaH_2PO_4 (pH 6.8). The assay was conducted in a 200 μL reaction system containing 148 μL of the buffer, 25 μL of diluted enzyme solution, and 2 μL of DMSO or sample (dissolved in DMSO). After 20 min of incubation in the 96-well plates at 37 °C, 25 μL of 0.4 mM 4-nitrophenyl-β-D-glucopyranoside (PNPG, Aladdin, Shanghai, China) was added as a substrate to start the enzymatic reaction. The plate was incubated for an additional 15 min at 37 °C, followed by the measurement of the optical density (OD). The final concentrations of tested compounds were between 0.39 and 100 μM. The OD was measured at an absorbance wavelength of 405 nm using a Microplate Reader (Tecan, Switzerland). All assays were performed in three replicates, and acarbose (Aladdin, Shanghai, China) was used as the positive control.

4. Conclusions

In conclusion, three new butenolide derivatives (**1**–**3**) and six known analogues (**4**–**9**) were isolated from the EtOAc extract of the strain *Aspergillus terreus* YPGA10, a fungus isolated from deep-sea sediments. The structures of compounds **1**–**3** were determined on the basis of comprehensive analyses of the NMR and MS data, and the absolute configurations of **1** and **2** were determined by comparisons of experimental ECD with calculated ECD spectra. Compound **1**, possessing a monosubstituted benzene ring, is rarely found in this group of butenolide derivatives. Compounds **6**–**9** exhibited remarkable inhibitory effects against *α*-glucosidase with IC_{50} values of 3.87, 1.37, 6.98, 8.06 μM, respectively, being much more active than the positive control acarbose (190.2 μM), which suggested that they could be developed as potential inhibitors of *α*-glucosidase.

Supplementary Materials: The following are available online at http://www.mdpi.com/1660-3397/17/6/332/s1, Figures S1–S29: ^{1}H, ^{13}C NMR, HSQC, ^{1}H-^{1}H COSY, HMBC, HRESIMS spectra of the new compounds **1**–**3**, ^{1}H and ^{13}C NMR of known compounds **4**–**9**.

Author Contributions: Z.C., Y.L., and W.L. isolated the compounds and elucidated the structures; L.L. and J.L. tested the inhibitions against *α*-glucosidase; W.X. and Z.L. isolated and identified the fungus and conducted the solid fermentation of the fungus; Q.L., W.Y., and Z.C. designed the study and edited the manuscript.

Funding: This work was supported by the grants from National Key R&D Program of China (2017YFD0600702-2), China Ocean Mineral Resources R&D Association (COMRA) Program (DY135-B2-09), First-Class Discipline Construction Project of Henan University (2018YLZDCG03), China Postdoctoral Science Foundation (2018M630815), and Start-Up Funding of Henan University (B2017067).

Acknowledgments: The authors thank Jianxun Kang at Zhengzhou University for NMR measurements and Ying Kang at Peking University for ECD calculations.

Conflicts of Interest: The authors declare no conflict of interest.

References

1. Parvatkar, R.R.; D'Souza, C.; Tripathi, A.; Naik, C.G. Aspernolides A and B, butenolides from a marine-derived fungus *Aspergillus terreus*. *Phytochemistry* **2009**, *70*, 128–132. [CrossRef] [PubMed]
2. He, F.; Bao, J.; Zhang, X.Y.; Tu, Z.C.; Shi, Y.M.; Qi, S.H. Asperterrestide A, a cytotoxic cyclic tetrapeptide from the marine-derived fungus *Aspergillus terreus* SCSGAF0162. *J. Nat. Prod.* **2013**, *76*, 1182–1186. [CrossRef] [PubMed]
3. Da Silva, I.P.; Brissow, E.; Kellner Filho, L.C.; Senabio, J.; de Siqueira, K.A.; Vandresen Filho, S.; Damasceno, J.L.; Mendes, S.A.; Tavares, D.C.; Magalhães, L.G.; et al. Bioactive compounds of *Aspergillus terreus* F7, an endophytic fungus from *Hyptis suaveolens* (L.) Poit. *World J. Microb. Biot.* **2017**, *33*, 62. [CrossRef] [PubMed]
4. Nuclear, P.; Sommit, D.; Boonyuen, N.; Pudhom, K. Butenolide and furandione from an endophytic *Aspergillus terreus*. *Chem. Pharm. Bull.* **2010**, *58*, 1221–1223. [CrossRef] [PubMed]
5. Zhang, Y.Y.; Zhang, Y.; Yao, Y.B.; Lei, X.-L.; Qian, Z.J. Butyrolactone-I from coral-derived fungus *Aspergillus terreus* attenuates neuro-inflammatory response via suppression of NF-κB pathway in BV-2 cells. *Mar. Drugs* **2018**, *16*, 202. [CrossRef] [PubMed]
6. Rao, K.V.; Sadhukhan, A.K.; Veerender, M.; Ravikumar, V.; Mohan, E.V.S.; Dhanvantri, S.D.; Sitaramkumar, M.; Moses Babu, J.; Vyas, K.; Om Reddy, G. Butyrolactones from *Aspergillus terreus*. *Chem. Pharm. Bull.* **2000**, *48*, 559–562. [CrossRef] [PubMed]
7. Haritakun, R.; Rachtawee, P.; Chanthaket, R.; Boonyuen, N.; Isaka, M. Butyrolactones from the fungus *Aspergillus terreus* BCC 4651. *Chem. Pharm. Bull.* **2010**, *58*, 1545–1548. [CrossRef] [PubMed]
8. Yang, L.-H.; Ou-Yang, H.; Yan, X.; Tang, B.W.; Fang, M.J.; Wu, Z.; Chen, J.W.; Qiu, Y.-K. Open-ring butenolides from a marine-derived anti-neuroinflammatory fungus *Aspergillus terreus* Y10. *Mar. Drugs* **2018**, *16*, 428. [CrossRef] [PubMed]
9. Sun, Y.; Liu, J.; Li, L.; Gong, C.; Wang, S.; Yang, F.; Hua, H.; Lin, H. New butenolide derivatives from the marine sponge-derived fungus *Aspergillus terreus*. *Bioorg. Med. Chem. Lett.* **2018**, *28*, 315–318. [CrossRef] [PubMed]
10. Liu, M.; Qi, C.; Sun, W.; Shen, L.; Wang, J.; Liu, J.; Lai, Y.; Xue, Y.; Hu, Z.; Zhang, Y. α-Glucosidase inhibitors from the coral-associated fungus *Aspergillus terreus*. *Front. Chem.* **2018**, *6*, 422. [CrossRef] [PubMed]
11. Munasaroh, S.R.; Tamat, S.; Dewi, R. Isolation and identification of α-glucosidase inhibitor from *Aspergillus terreus* F38. *Indones. J. Pharm.* **2018**, *29*, 74–79. [CrossRef]
12. Skropeta, D.; Wei, L. Recent advances in deep-sea natural products. *Nat. Prod. Rep.* **2014**, *31*, 999–1025. [CrossRef] [PubMed]
13. Cheng, Z.; Xu, W.; Wang, Y.; Bai, S.; Liu, L.; Luo, Z.; Yuan, W.; Li, Q. Two new meroterpenoids and two new monoterpenoids from the deep sea-derived fungus *Penicillium* sp. YPGA11. *Fitoterapia* **2019**, *133*, 120–124. [CrossRef] [PubMed]
14. Liu, L.; Xu, W.; Li, S.; Chen, M.; Cheng, Y.; Yuan, W.; Cheng, Z.; Li, Q. Penicindopene A, a new indole diterpene from the deep-sea fungus *Penicillium* sp. YPCMAC1. *Nat. Prod. Res.* **2018**, *Oct 1*, 1–7. [CrossRef]
15. Cheng, Z.; Xu, W.; Liu, L.; Li, S.; Yuan, W.; Luo, Z.; Zhang, J.; Cheng, Y.; Li, Q. Peniginsengins B–E, new farnesylcyclohexenones from the deep sea-derived fungus *Penicillium* sp. YPGA11. *Mar. Drugs* **2018**, *16*, 358. [CrossRef] [PubMed]
16. Cheng, Z.; Zhao, J.; Liu, D.; Proksch, P.; Zhao, Z.; Lin, W. Eremophilane-type sesquiterpenoids from an *Acremonium* sp. fungus isolated from deep-sea sediments. *J. Nat. Prod.* **2016**, *79*, 1035–1047. [CrossRef] [PubMed]
17. Li, Y.; Liu, W.; Xu, W.; Zeng, X.; Cheng, Z.; Li, Q. Aspterrics A and B, new sesquiterpenes from deep sea-derived fungus *Aspergillus terreus* YPGA10. *Rec. Nat. Prod.* **2019**. [CrossRef]

18. Lin, T.; Lu, C.; Shen, Y. Secondary metabolites of *Aspergillus* sp. F1, a commensal fungal strain of *Trewia nudiflora*. *Nat. Prod. Res.* **2009**, *23*, 77–85. [CrossRef] [PubMed]
19. *Sybyl Software*, version X 2.0; Tripos Associates Inc.: St. Louis, MO, USA, 2013.
20. Frisch, M.J.; Trucks, G.W.; Schlegel, H.B.; Scuseria, G.E.; Robb, M.A.; Cheeseman, J.R.; Scalmani, G.; Barone, V.; Petersson, G.A.; Nakatsuji, H.; et al. *Gaussian 09, Rev. C 01*; Gaussian, Inc.: Wallingford, CT, USA, 2009.
21. Boue, S.M.; Daigle, K.W.; Chen, M.-H.; Cao, H.; Heiman, M.L. Antidiabetic potential of purple and red rice (*Oryza sativa* L.) bran extracts. *J. Agric. Food Chem.* **2016**, *64*, 5345–5353. [CrossRef] [PubMed]
22. Omar, R.; Li, L.; Yuan, T.; Seeram, N.P. α-Glucosidase inhibitory hydrolyzable tannins from *Eugenia jambolana* seeds. *J. Nat. Prod.* **2012**, *75*, 1505–1509. [CrossRef] [PubMed]